Available online at www.eccomasproceedia.org
Eccomas Proceedia COMPDYN (2023) 1563-1570

ECCOMAS
Proceedia

COMPDYN 2023
9th ECCOMAS Thematic Conference on
Computational Methods in Structural Dynamics and Earthquake Engineering
M. Papadrakakis, M. Fragiadakis (eds.)
Athens, Greece, 12-14 June 2023

FINITE ELEMENT ANALYSIS OF HIGH DAMPING UNBONDED FIBER REINFORCED ELASTOMERIC ISOLATORS (UFREIS) OF DIFFERENT SHAPE FACTORS

Gaetano Pianese[1], Gabriele Milani[1], and Antonio Formisano[2]

[1] Politecnico di Milano
Piazza Leonardo da Vinci 32, 20133 Milano, Italy
e-mail: {gaetano.pianese, gabriele.milani}@polimi.it

[2] School of Polytechnic and Basic Sciences "Federico II"
Piazzale Tecchio 80, 80125 Napoli, Italy
antonio.formisano@unina.it

Abstract

Losses and damages induced by earthquakes are a dramatic reality worldwide. Consequently, implementing innovative protection strategies for existing and new constructions is of societal importance. Elastomeric isolators are special devices for the seismic isolation of structures. Typically, they are made of layers of steel laminas and rubber, and they are interposed between the ground and the structure to increase the natural period and reduce the inertia forces to apply in case of an earthquake. Fiber-reinforced elastomeric isolator (FREI) is a new type of elastomeric isolator. Instead of steel laminas, thin fiber layers are used for vertical reinforcement. Compared with the steel-reinforced ones, FREIs have considerably lower weight and can be manufactured through cold vulcanization. They can be applied to the structure in several methods: bonded, unbonded, partially bonded, and friction (no bonding between rubber and fiber layers). In unbonded applications (UFREI), the isolators can simply be installed between the upper structure and foundation without bonding or fastening. So, the shear load is transferred through the friction generated between the UFREI and the structure surfaces, improving the dissipation energy of the device. This study proposes a detailed 3D finite element modeling of UFREIs, considering different shape factors. The devices, made of high-damping rubber and glass fiber-reinforced polymer laminas, have been subjected to a cyclic horizontal displacement up to 150% of the total height of the rubber pads under constant vertical pressure. Results evaluated in terms of horizontal stiffness, damping ratio, and horizontal period have highlighted the significant influence of the shape factors on the final lateral response of the UFREIs.

Keywords: Base Isolation, Fiber-Reinforced Elastomeric Isolator, High-Damping Rubber, Finite Element Analysis, Shape Factors.

ISSN:2623-3347 Published by Eccomas Proceedia.
Peer-review under responsibility of the organizing committee of COMPDYN 2023.
doi: 10.7712/120123.10501.20161

1 INTRODUCTION

Fiber-Reinforced Elastomeric Isolators (FREIs) are a new type of elastomeric device able to isolate structures from ground motions during earthquakes [1], consisting of rubber pads alternating with thin fiber layers instead of steel lamina used in the traditional Steel Reinforced Elastomeric Isolators (SREIs). They can be used in various applications, including bridges [2], buildings [3], and other civil engineering structures. One particular application of FREIs is the unbonded configuration (UFREI), where the isolator is placed between the superstructure and substructure without any bonding or fastening [4–6]. The UFREI offers several advantages, such as low-cost installation [7–9] and ease of replacement. Moreover, the UFREI effectively reduces the seismic forces transmitted to the superstructure. In fact, during horizontal displacements, it results in a stable roll-over lateral deformation, which reduces the horizontal stiffness and increases the efficiency of the devices (Figure 1). Furthermore, compared to the identical specimen but in bonded conditions, the UFREIs result in superior performance concerning the damping ability [5].

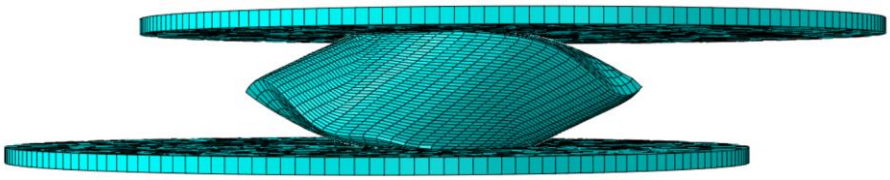

Figure 1: UFREI roll-over deformation

The performance of UFREIs depends on several factors, such as the geometrical properties [10]. Two shape factors can describe these geometrical properties: the first shape factor, S_1, is determined as the ratio of the plan area to the free-to-bulge area of a single elastomer layer; the second shape factor, S_2, equal to the ratio of the bearing width to the overall thickness of the elastomer layers. This study proposes a numerical investigation of three different models of UFREIs, conceived by the authors for base seismic isolation of low-rise masonry buildings in developing countries where shape factors vary. The final aim is to evaluate their influence on the UFREI lateral response, assessed in terms of horizontal stiffness, horizontal period, and damping ratio.

2 HIGH-DAMPING RUBBER COMPOUND (NR-EPDM)

The first part of the study has focused on the rubber compound characterization. A high-performance rubber composition (good durability and cyclic dissipation) made of a Natural Rubber and Ethylene Propylene Diene Monomer (NR-EPDM) blend has been proposed. The rubber compound behavior has been characterized by various experimental tests. Results are summarized in Table 1, Table 2, and Table 3. Mechanical and physical properties have met the minimum requirements of table 9 of UNI EN 15129 (minimum requirements for high-damping rubber compounds for elastomeric isolators).

Density	Hardness	Tensile Strenght at break	Elongation at break	Young Modulus	Tear Resistance
[g/cm^3]	[IRHD]	[MPa]	[%]	[MPa]	[kN/m]
1.129	59.98	16.06	613.0	1.63	22.84

Table 1: Mechanical and physical properties of rubber compounds

Accelerated air oven aging			Compression
Δ H	Δ TS_{break}	Δ E_{break}	Set
[IRHD]	[%]	[%]	[%]
1.00	-4.51	-9.51	35

Table 2: Results of the rubber compounds after accelerated aging and compression set

Numerical		Experimental																	
		Fresh		Aged		Frequency				Temperature									
ξ	G Modulus	ξ	G Modulus	Δξ	ΔG	0.1Hz		2.0 Hz		40°C		0°C		(-10°C)		(-15°C)	
						Δξ	ΔG	Δξ	ΔG	Δξ	ΔG	Δξ	ΔG	Δξ	ΔG	Δξ	ΔG
[%]	[MPa]	[%]	[MPa]	[%]	[%]	[%]	[%]	[%]	[%]	[%]	[%]	[%]	[%]	[%]	[%]	[%]	[%]
8.49	0.70	8.38	0.77	-12	+19	+2	+1	+4	-6	+10	-15	+12	+30	+29	+47	+45	+68

Table 3: Numerical and experimental shear test results

Uniaxial tensile and relaxation tests have been performed to obtain the hyperelastic and viscoelastic properties of the NR-EPDM rubber compound. Such experimentation was crucial to correctly define a Finite Element (FE) model that has been used to simulate the cyclic shear behavior for the rubber first (validation) and later for the complete device. The experimental values have been inserted on the FE software code Abaqus [11] to be fitted with the Yeoh model (hyperelasticity) and the Maxwell model (viscoelasticity) (Figure 2). The rubber hyperelastic and viscoelastic coefficients obtained are shown in Table 4 and Table 5.

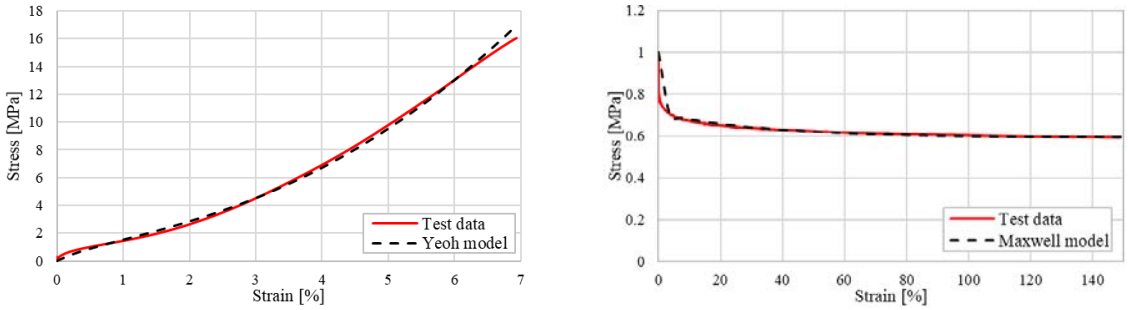

(a) (b)

Figure 2: Comparison between experimental data and numerical model: Yeoh (a) and Maxwell (b)

C_{10}	C_{20}	C_{30}	D
0.411327320	6.170050466E-03	-7.890913554E-06	0

Table 4: Yeoh model coefficients

g_1	τ_1	g_2	τ_2
0.29131	0.17077	0.11519	35.303

Table 5: Maxwell model (Prony Series) coefficients

Then, the rubber shear test has been modeled, and the analysis has been performed (Figure 3a). The quadruple shear specimen has been subjected to four complete 0.5 Hz cyclic horizontal displacements up to 20 mm (100% rubber pad thickness).

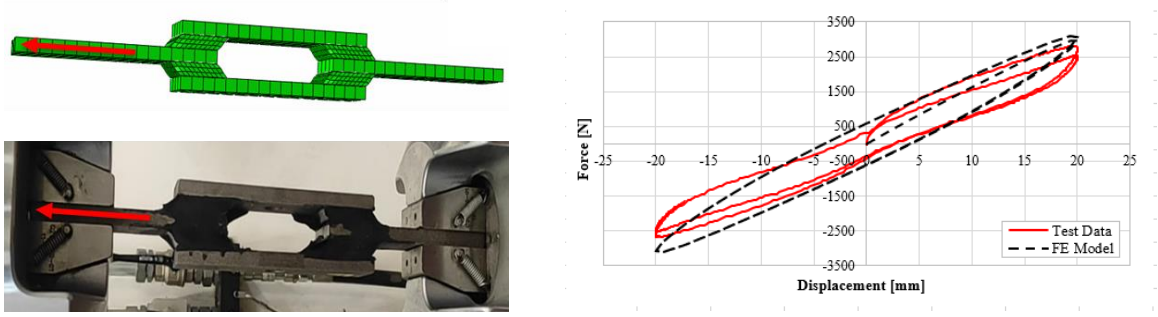

(a) (b)

Figure 3: Quadruple shear test numerical model and experimental setup (a); numerical and experimental displacement-force curves (b)

The shear modulus (G) and damping (ξ) values have been evaluated for the third deformation cycle based on the following equations:

$$k_H = (F_{max} - F_{min})/(\Delta_{max} - \Delta_{min}) \quad (1)$$

$$\xi = W_d/(4\pi W_s) \quad (2)$$

$$W_S = (1/2) * k_H * \Delta^2 \quad (3)$$

$$\Delta = (\Delta_{max} + \Delta_{min})/2 \quad (4)$$

$$G = k_H * (t/A) \quad (5)$$

where k_H is the horizontal stiffness; F_{max} and F_{min} are, respectively, the maximum and minimum forces; Δ_{max} and Δ_{min} are respectively the maximum and minimum displacements; W_d is the area within the curve (dissipated energy); W_s is the restored energy; t and A are respectively the thickness and the area of the rubber pads (quadruple shear specimens). The numerical results are in good agreement with the experimental ones (Figure 3b and Table 3). So, the parameters reported in Table 4 and Table 5 have been considered for the numerical analysis of the UFREIs, the subject of the next section.

3 FINITE ELEMENT ANALYSIS

3.1 UFREI model

The device object of the study is a circular UFREI, constituted by alternating layers of rubber pads (made of NR-EPDM) and Glass Fiber Reinforce Polymer (GFRP) laminas. In Figure 4 and Table 6, the geometrical characteristics of UFREIs are shown. The base (b), the thickness of GFRP laminas (T_f), and the total thickness of the rubber (T_{rtot}) are common parameters for the three models proposed. The first shape factor (S_1), evaluated as the ratio between the area (A) and the lateral area of the single rubber layer ($C*T_r$), decreases from UFREI200A to UFREI200C. Instead, the second shape factor (S_2), evaluated as the ratio between the base (b) and the total height of the device (h), increases from UFREI200A to UFREI200C.

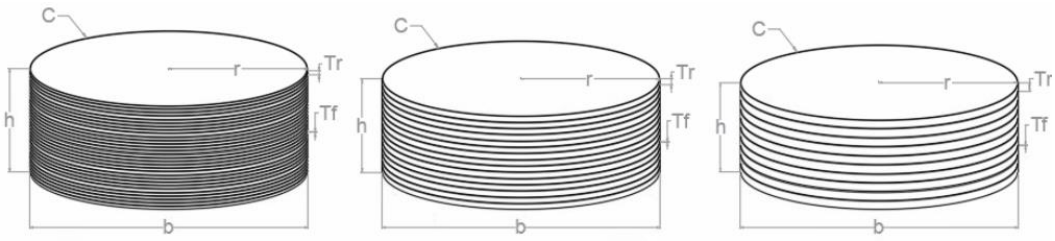

Figure 4: Proposed design of the circular FREIs: FREI200A (Left), FREI200B (Center), FREI200C (Right)

Model	H	b	C	A	T_r	T_f	rubber layers	fiber laminas	T_{rtot}	T_{ftot}	S_1	S_2
[-]	[mm]	[mm]	[mm]	[mm^2]	[mm]	[mm]	[-]	[-]	[mm]	[mm]	[-]	[-]
200A	74.5	200	628.32	31415.92	2	0.5	30	29	60	14.5	25.00	2.68
200B	67	200	628.32	31415.92	4	0.5	15	14	60	7	12.50	2.98
200C	64.5	200	628.32	31415.92	6	0.5	10	9	60	4.5	8.34	3.10

Table 6: Geometrical characteristics of the circular UFREIs

The UFREIs have been modeled in Abaqus using eight-node brick elements (C3D8H) [12]. The final mesh is shown in Figure 5. There is no bonding between the supports and the rubber pad. So, a penalty surface-interaction model has been introduced between the two surfaces, and a friction coefficient of μ=1 has been applied [5]. GFRP laminas have been modeled as embedded regions in the rubber device. Yeoh and Maxwell models have been used to represent the rubber behavior as described in the previous section. The fiber has been assumed isotropic-elastic with a Young modulus of E=10000 MPa and a Poisson ratio υ=0.2.

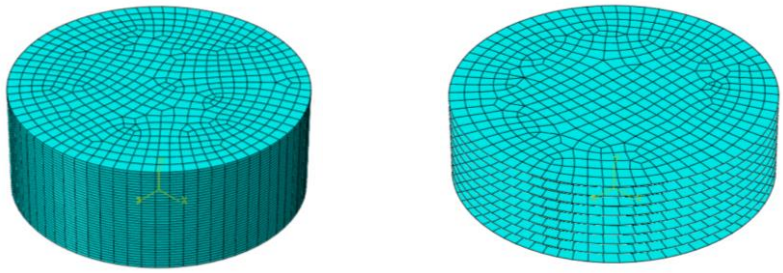

(a) (b)

Figure 5: Rubber (a) and GFRP laminas (b) final mesh (UFREI200C).

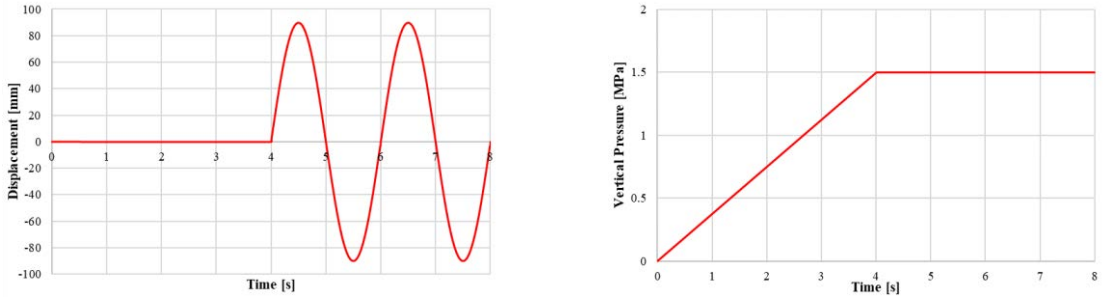

(a) (b)

Figure 6: Cyclic horizontal displacement amplitude (a) and vertical pressure (b)

The UFREIs have been subjected to a 0.5 Hz cyclic horizontal displacement up to 90 mm (Figure 6a) (150% t_r), applied at the top support, under constant vertical pressure of 1.5 MPa, i.e. the expected working pressure (Figure 6b).

3.2 Results

Effective horizontal stiffness K_{Heff}, damping ratio ξ, and horizontal period T_h have been evaluated. The computations are based on Equations (6)-(11), where f_h is the horizontal frequency, g is the gravitational acceleration, and p is the vertical pressure. In the following figures and table, the numerical results are shown.

$$K_{H,eff} = (F_{max} - F_{min})/(\Delta_{max} - \Delta_{min}) \quad (6)$$

$$\xi = W_d/(4*\pi*W_s) \quad (7)$$

$$Ws = (1/2)*K_{H,eff}*\Delta^2_{max,ave} \quad (8)$$

$$\Delta_{max,ave} = (\Delta_{max} + \Delta_{min})/2 \quad (9)$$

$$f_h = ((K_h*g)/(p*A))^{0.5}/(2*\pi) \quad (10)$$

$$T_h = 1/f_h \quad (11)$$

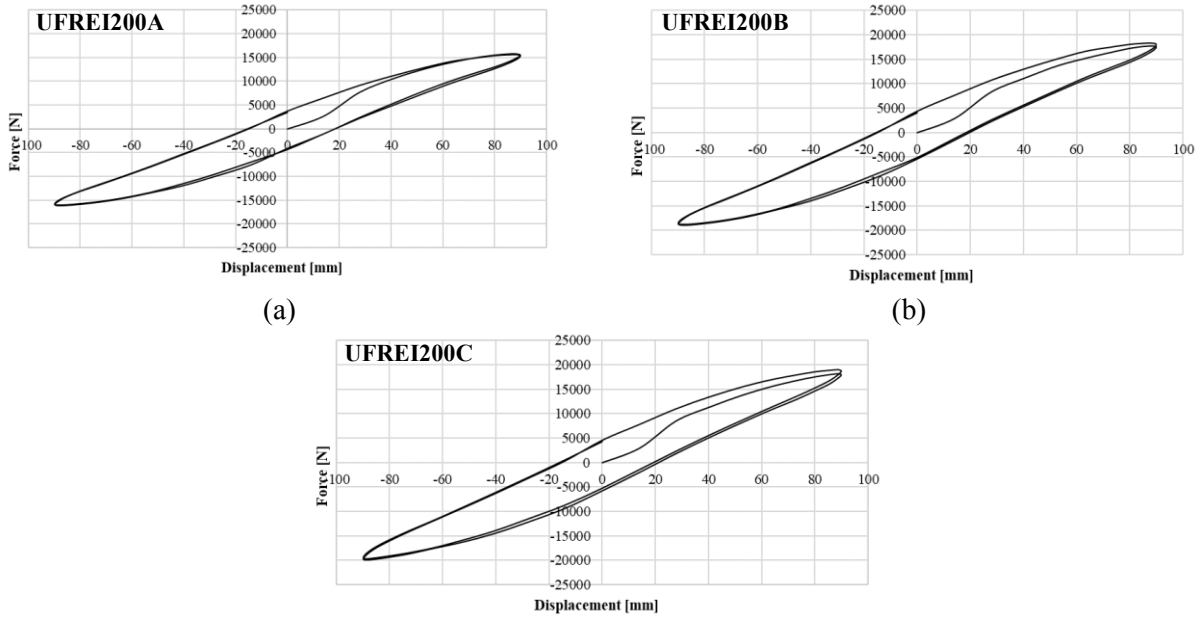

(a) (b)

(c)

Figure 7: Force-Displacement curves for UFREI200A (a), UFREI200B (b), and UFREI200C (c)

		UFREI200A	UFREI200B	UFREI200C
K_h	[N/mm]	175.20	206.12	215.04
ξ	[%]	10.53	11.02	11.18
f_h	[Hz]	0.96	1.04	1.06
T_h	[s]	1.04	0.96	0.94
$F_{h,\,max}$	[N]	15954.2	18769.7	19028.3

Table 7: Numerical results

4 CONCLUSIONS

In this paper, the influence of shape factors on the final lateral response of UFREIs has been investigated. First, the rubber compound has been characterized through several experimental tests. All the mechanical and physical properties of the NR-EPDM rubber blend proposed have met the minimum requirements of the UNI EN 15129 code for high-damping rubber compounds for elastomeric isolators. Subsequentially, uniaxial tensile and relaxation tests have been performed to obtain the hyperelastic and viscoelastic properties of the rubber pads for the 3D FE model. The experimental values have been inserted on the FE software code Abaqus to be fitted with the Yeoh model (hyperelasticity) and the Maxwell model (viscoelasticity). Comparing the experimental and numerical results of the shear test has confirmed the reliability of the numerical parameters considered. In the second part, UFREIs are presented. Three models with different shape factors have been proposed. FE cyclic shear tests have been carried out by subjecting the UFREIs to a cyclic horizontal displacement up to 150% of the total height of the rubber pads under constant vertical pressure of 1.5 MPa. Numerical results, in terms of horizontal stiffness, damping ratio, and horizontal period, demonstrate the impact of the shape factors on the final lateral response of the UFREIs. Specifically, decreasing the first shape factor increases the horizontal stiffness and damping ratio and reduces the horizontal period. Conversely, increasing the second shape factor decreases the horizontal stiffness and damping ratio and increases the horizontal period.

These results provide valuable insights into the design and optimization of UFREIs. However, additional experimental tests are under investigation by the authors. This will not only enhance the accuracy of the model but also facilitate the practical implementation of UFREIs in future civil engineering applications.

REFERENCES

[1] van Engelen, N. C., 2019, “Fiber-Reinforced Elastomeric Isolators: A Review,” Soil Dynamics and Earthquake Engineering, **125**.

[2] Al-Anany, Y. M., and Tait, M. J., 2017, “Fiber Reinforced Elastomeric Isolators for the Seismic Isolation of Bridges,” Compos Struct, **160**.

[3] Habieb, A. B., Valente, M., and Milani, G., 2019, “Base Seismic Isolation of a Historical Masonry Church Using Fiber Reinforced Elastomeric Isolators,” Soil Dynamics and Earthquake Engineering, **120**.

[4] Ehsani, B., and Toopchi-Nezhad, H., 2017, “Systematic Design of Unbonded Fiber Reinforced Elastomeric Isolators,” Eng Struct, **132**, pp. 383–398.

[5] Toopchi-Nezhad, H., Tait, M. J., and Drysdale, R. G., 2011, “Bonded versus Unbonded Strip Fiber Reinforced Elastomeric Isolators: Finite Element Analysis,” Compos Struct, **93**(2).

[6] Russo, G., and Pauletta, M., 2013, “Sliding Instability of Fiber-Reinforced Elastomeric Isolators in Unbonded Applications,” Eng Struct, **48**, pp. 70–80.

[7] Habieb, A. B., Milani, G., Tavio, and Milani, F., 2017, “Seismic Performance of a Masonry Building Isolated with Low-Cost Rubber Isolators,” *WIT Transactions on the Built Environment*.

[8] Habieb, A. B., Milani, G., Tavio, T., and Milani, F., 2021, “Seismic Protection of Unreinforced Masonry Buildings by Means of Low Cost Elastomeric Isolation Systems,” International Journal of Masonry Research and Innovation, **6**(2).

[9] Tavio, T., Milani, F., Habieb, A. B., and Milani, G., 2020, “Seismic Protection of Unreinforced Masonry Buildings by Means of Low Cost Elastomeric Isolation Systems,” International Journal of Masonry Research and Innovation, **1**(1).

[10] Toopchi-Nezhad, H., Tait, M. J., and Drysdale, R. G., 2013, "Influence of Thickness of Individual Elastomer Layers (First Shape Factor) on the Response of Unbonded Fiber-Reinforced Elastomeric Bearings," J Compos Mater, **47**(27).
[11] Smith, M., 2020, *ABAQUS/Standard User's Manual, Version 6.9*.
[12] Pianese, G., Milani, G., and Formisano, A., 2021, "FE Modeling of a Seismic Isolator Made of HDR and Regenerated EPDM," *COMPDYN Proceedings*.